

JUST PUSH PRINT

Biodevice Printing Using Bioinks, Electroinks and Quantum Dot Inks

Jan Lawrence Sumerel and Kai Sudau

FUJIFILM Dimatix, Inc., 2230 Martin Avenue, Santa Clara, California 95050-2704, U.S.A.

Keywords: Ink jet, piezoelectric, biomaterials, microarray, bioink, electroink, quantum dot.

Abstract: Many advanced medical and environmental test devices require microscale patterning of cells, proteins, or other biological materials, and the need for these devices to contain active functional material components has increased dramatically. In addition, the biological material oftentimes requires an interface with an electrical or optical output signal. Efficient production methods are paramount to meeting market demands, and ink jet printing offers an easy, low cost alternative to materials deposition used in current biodevice manufacturing. However, fluid development and proper printing parameters at the research level are required for manufacturing processing and will be critical to process adoption. In this paper, operating parameters and fluid characterization have been developed through processing biomaterials, organic and inorganic conductive fluids and semiconductor nanoparticles. Because of the inherent versatility, uniformity and scalability of this system, established operating parameters coupled with proper fluid characterization will ultimately be translatable to production line systems of biodevice components.

1 INTRODUCTION

Biological monitoring devices and medical devices generally have two material components used in a stepwise fashion, a biological material that works as both a reaction beacon and the biochemical reactive site followed by an optical, piezoelectric or electronic material that amplifies the signal to allow a measurable readout of the reaction. Typically, manufacturing protocols are distinct for each component, but ink jet printing can be used for the deposition of both materials. Interfacing processing of these two components may be critical to biodevice success, and electronic file pattern formation allows component alignment. Ink jet printing is inherently compatible to high throughput (Antoniadis, 2007). Already, interesting technological phenomena have spawned from the patterning of structurally and functionally different materials including high performance ceramics (Lewis, et al, 2006). For this reason, drop-on-demand ink jet printing, a simple fabrication process, has become a prominent player in materials processing for biodevice components (Padinger, 2007). However, it is a big step for biodevice developers to jump into robust in-line manufacturing production systems. This type of equipment

requires a sizable financial investment plus sufficient experience so that manufacturing specifications and in-house knowledge can be established. Thus, a low cost, easy-to-use laboratory scale system is required for preliminary experimentation. This strategy then allows substrate evaluation, on-site development, and fluid manufacturing to all occur simultaneously. This need has been addressed with an R&D tool that offers printhead maintenance, substrate alignment, nozzle inspection and drop analysis, and ease-of-use (Sumerel et al, 2006).

Just push print, the most common command for the desktop printer, can now be used in the laboratory or in manufacturing lines. Ink jet printing is a simple and cost effective technique with applications in the fields of electronics and biomedicine and has been shown to have specific applications in these industries (Sirringhaus et al., 2000, Calvert, 2001, Haber et al., 2005). In contrast to other multi-step production methods, ink jet printing is an additive process that precisely deposits metered quantities of fluid onto a variety of substrates including glass, silicon, plastics, organic thinfilms, and metals based on a user generated pattern. The resolution of the printed pattern is determined by a number of factors, including

substrate/fluid contact angle, nozzle size, and lateral resolution of the printhead (Song and Nur, 2004). Ink jet printers can dispense fluid drops with volumes in the picoliter (ρL) to microliter (μL) range, and an integral step in bringing this processing technique from the laboratory to manufacturing systems is the development of jettable fluids. The chemical properties of the fluid, including density, surface tension and viscosity, determine its jettability (Sumerel, et al., 2006). During drop formation, energy is distributed between the fluid's viscous flow, surface tension, and kinetic energy (Xu et al., 2005). The deposited fluid volume is directly proportional to nozzle size. This flexibility enables microscopic patterned thinfilms of functional materials at a variety of resolutions. The physical properties of the patterned thinfilms (film thickness and pixel values) are dependent on the fluids coupled with the drive electronics of the printing device. In general, 2D drawings, pictures or structures, formatted as a bitmap image, can be translated into X and Y print coordinates for materials deposition (drop-on-demand). Each individual nozzle ejects a drop with a ligament. The ligament and the drop coalesce during flight to make a volumetric sphere and upon contact with the substrate, the sphere alters its three dimensional structure to become columnar. The resulting printed image is a compilation of drops where the third dimension is equal to film thickness, a physical property that is dependent on particle loading, drop spacing and drop spread. Once this critical but iterative R&D phase of process and material evaluation is complete to allow sustainable ink jet printing, the fluids are scalable for production use.

1.1 Ink Jet Printing Employing MEMS Devices

The required heating process for thermal ink jet printing (300°C) will damage thermally-sensitive materials, thereby limiting their use in devising functional devices (Calvert, 2001, Xu et al., 2005). In contrast, using piezoelectric ink jet printing, thermally sensitive materials are deposited under ambient conditions. Piezoelectric printheads contain a lead zirconate titanate (PZT) piezoelectric ceramic, nozzles, and a fluid chamber. When a voltage is applied to the PZT, mechanical vibrations create acoustic waves that in turn force fluid out of the chamber through the nozzles (Brünahl and Grish, 2002). Piezoelectric printheads are categorized based on the deformation mode of the PZT (e.g.,

squeeze mode, bend mode, push mode, or shear mode) (Myatt et al., 2006). MEMS fabrication has increased the precision and resolution of the deposited materials (Menzel, C., 2005). These silicon devices increase jet-to-jet uniformity and drop placement accuracy. The inertness of the silicon expands the operating ranges to allow higher chemical diversity and fluid throughput expanding piezoelectric ink jet printing from the ability to print graphic inks to the realm of printing functional fluids required for biodevice manufacturing.

The ink jet printhead is powered by a piezoelectric unimorph, which is constructed in the plane of the wafer and consists of patterned PZT bonded to a silicon diaphragm (Brünahl and Grish, 2002). The effective diameter of the nozzle is 21.5 μm ; this nozzle size is approximated to generate 10 ρL drops. An important operating parameter of this particular device is the negligible void volume due to the direct fluid/printhead interface.

Fluid flow properties like low viscosities, low boiling points, high surface tensions and non-Newtonian behaviors are hallmarks of functional materials and are also generally unfavorable chemical characteristics for ink jet printing. Manipulating the parameters that generate the electronic signal to drive the movement of the PZT, including its frequency, wave shape, wave duration and voltage has provided a significant advancement in printing an array of functional materials and has been one of the areas of our research. The ability to adjust the jetting parameters has been critical to the success of printing bioinks and electroinks.

1.2 Functional Fluid Deposition

Thermal ink jet printing has been employed for the deposition of biomaterials (Xu et al, 2005, Setti et al., 2005). A glucose biosensor was fabricated by thermal ink jet printing, and the enzyme, glucose oxidase was made into a biological ink using phosphate buffer and 10% glycerol (Setti et al., 2005). In contrast to piezoelectric ink jet printing where there are requirements for viscosity (8-14 centipoise (cps)) and surface tension (28-32 dynescm⁻¹), most biological materials exhibit very low viscosities (1 cps) and very high surface tension values (60 dynescm⁻¹). In addition, biological fluids generate steam at high temperatures just like inks in thermal ink jet printers. This heating process causes bubble formation and fluid output at the nozzle plate (Bae, et a., 2005). Major fabrication advances have been made using thermal ink jet printing (Lemmo et al., 1998) due to the low cost and wide availability,

and at first glance this method should simplify biomaterials deposition due to the looser requirements for fluid formulation. However, the thermal ink jet process may cause damage to thermally-sensitive materials used in biology and medicine. In contrast, piezoelectric ink jet printing is a thermally constant process and does not require heat thereby increasing the chances of biomaterial stability.

Rapid detection employing microarray methods are necessary to biomedical and chemical sciences (Diehl, F., 2002). Miniaturization and automation of arrays may lead to decreased costs and faster analysis times (Peck, 2007). As drop sizes decrease, feature sizes decrease and array densities increase. Many forensic samples obtained in the field have restricted amounts of recoverable material, and in some cases, two polymerase chain reactions are required to reach the levels of sensitivity and verification required in the amplified deoxyribonucleic acid (DNA) product (Vuorio et al., 1990). Since piezoelectric ink jet printing only requires 10 μ L per sample, the amount of DNA needed for a precise polymerase chain reaction assay is greatly reduced. For example, this technique may provide an important advance in studying the variation in a segment of mitochondrial DNA (a non-coding region between two transfer ribonucleic acid genes) (Salas et al., 2001). Variations in this section of the gene is one obvious choice for forensic identification because of sample number (Wilson et al., 1995), and the predominant isolated sample, human hair, shows low keratin protein variation between individuals (Rodriguez-Calvo et al., 1992). Unlike contact printing techniques (e.g., pin spotters) or expensive industrial ink jet printheads, the single-use ink jet printhead technology requires minimal deposition of fluids and minimal cross-contamination (Manning, H., 2007).

The need for continual reiterations of circuit design gestures for new approaches away from the reductive process of masking and etching to create metal patterns (Hwang, 2002) towards additive processing. There are also market drivers for organic electronic materials due to their adherence to substrates, flexibility, performance and the ability to process these materials at low temperatures (Shaw and Seidler, 2001). Ink jet printing provides the necessary technological platform to increase throughput and lower processing costs. Indeed, low capital costs, process simplicity, and flexibility have been the important attributes that make this technique practical for conductive trace patterning. Many conductive precursor fluids are being jetted

using both thermal and piezoelectric ink jet printers (Sirringhaus et al., 2000, Sawhney et al., 2006, Teng and Vest, 1988; Volkman, et al., 2004). In fact, ink jet printing is considered one of the key technologies in defined polymer deposition (Sawhney, 2006). Polymer structural confirmation varies with temperature thus ambient processing conditions are required. At low temperatures, typically below the glass transition temperature (T_g), polymers maintain their natural, globular structure. At higher temperatures, above the T_g , they swell into open conformations, essentially breaking their entropically favorable π - π interactions (Baiesi et al., 2001). With the conformational collapse, the material becomes less conductive. In order to move towards feasible ink jet manufacturing processes for either conductive polymers or metallo-organic fluids, initiating formulation, printing and post-processing techniques are required. The fluids must maintain solvent monodispersity; once printed, they must properly adhere to the surface (Mei et al., 2005). These criteria are integral for successful printing, for even the smallest amount of discontinuity will make the material non-conductive and lower its mechanical strength.

Early attempts at ink jet printing silver metallo-organic fluids capitalized on its advantageous annealing temperature post-printing (200°C). The resultant silver conductive traces on a variety of materials including flexible substrates and substrates are left with a low thermal budget (Volkman et al., 2004). The direct writing of silver ink onto a grid pattern of solar cells has been previously done using a self-built printer and a Siemens ink jet printhead (Teng and Vest, 1988). They modified their printhead by machining restrictive nozzle plates that varied drop size. The printer was run between 100 and 200 Hz which resulted in a printing speed of a few cmsec⁻¹. This single laboratory technique was a slow throughput process and required multiple printing cycles for effective deposition, so although it is not agreeable to manufacturing protocols, it was an important proof of concept step.

The choice of additional organic material in the starting fluid greatly influences the obtained conductivity (Mei et al., 2005). Once printed, the silver in the fluid must be annealed to convert the nanoparticles to a bulk silver thinfilm so that the resistance values can closely mimic bulk silver. The resulting amount of silver per volume of fluid is controlled by the annealing temperature cycle controls, and the effect of the organic decomposition into the gas phase during annealing determines the porosity of the printed material, which affects its

continuity (Mei et al., 2005). Additionally, the proper jetting parameters required for high performance printing is fundamental for reproducible deposition. The final feature size of the material on the substrate is determined by these parameters, and the overall conductivity is established according to the applied thermal processing (Mei et al., 2005).

2 MATERIALS AND METHODS

Proteins were dissolved in phosphate buffer saline solution (Fisher Scientific, Fair Lawn, NJ, USA) and 1.6 μM solution. 1 % of polysorbate 20 surfactant (Fisher Scientific, Fair Lawn, NJ, USA). 10 mg/mL of human genomic DNA was dissolved in 50% ethanediol.

Two percent (2%) glycerol (Sigma Aldrich, St. Louis, MO) was added to a poly (3,4-ethylenedioxythiophene) poly(styrenesulfonate) (PEDOT/PSS) aqueous dispersion (H.C. Stark, Goslar, Germany). ANP Silverjet nanopaste (Advanced Nanoproducts, Chungcheonguk-do, Korea) and Cabot Inkjet Silver Conductor (Ag-Ij-G-100-S1, Albuquerque, NM) were used as packaged. Fluids were sonicated in a water bath in a Branson 1510 sonicator at room temperature using highest sonic level for 30 minutes. Fluids were degassed for 2 hours at 5 mbar pressure in a degassing chamber.

Quantum dots were obtained from UT Dots (Savoy, IL, USA) and were serially diluted in 53% polypropylene glycol 400, 45% propylene carbonate solution containing 0.01% tetramethyl-5-decyne-4,6-diol, 2,4,7,9-propanol (Surfynol 104PA; Air Products, Allentown, PA).

Clean glass wafers were purchased from VWR (VWR Scientific, West Chester, PA). Both Kapton[®] (Dupont, Wilmington, DE) and Teslin[®] synthetic thinfilms (PPG Industries, Pittsburgh, PA) were kept clean after purchasing and cut into 8 x 11 inch sheets using laboratory scissors that had been cleaned with 70% ethanol (Sigma-Aldrich, St. Louis, MO). Single-side polished 150 mm silicon 100 wafers were obtained from Silicon Quest International (Santa Clara, CA) and sputtered with 300 nm gold layer using an Au target and a converted TES sputterer.

The DMP-2831 (FUJIFILM Dimatix, Santa Clara, CA) was used according to packaging instructions. Contact angle measurements were carried out using a VCA Optima XE (AST, Billerica, MA). 2 μL samples were manually pipetted for the measurements.

Scanning electron micrographs were obtained using a Philips XL30 ESEM. Resolution was obtained based on operating voltage of 5 kV.

Tapping mode AFM was conducted on a Digital Instruments Dimension 3100 using an etched silicon tip with a nominal radius of curvature of 10 - 20 nm. Scan sizes were varied, depending on the feature size. The scan rate was 0.1 - 0.3 Hz. The set point was set to 60 - 70% of the free-standing root mean square of the voltage of the oscillating tip.

Resistance measurements were obtained using a Fluke 110 True RM multimeter. Anode was put at one end of silver contact on glass wafer and cathode was placed on top of other end of silver contact. Electrodes were manually held during measurements.

3 DISCUSSION

Both DNA and proteins were ink jet printed after fluid formulation trials. Human genomic deoxyribonucleic acid was printed in 10 μL of 50% ethanediol in the bottom of a 384 well assay plate or onto a silicon wafer in a 254 μm grid with high fidelity drop formation and uniform drop speed (Figure 1). The high surface tension of the DNA in water was mediated by the lower surface tension of the 1,2 ethanediol (47 dynescm⁻¹) but the short ligaments in Figure 1 demonstrated how the surface tension of the fluid is still the predominant force in drop formation.

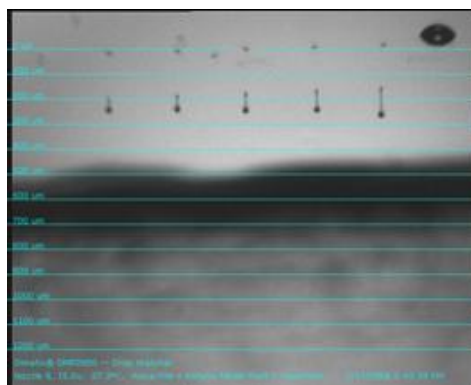


Figure 1: Deoxyribonucleic acid leaving the nozzle plate.

The only way to successfully print this fluid was by lowering the jetting frequency and extending the wave pulse from 11.52 μs to 14.1 μs . After successful printing, the samples were air-dried and tested for polymerase chain reaction amplification. A 750 base pair fragment was resolved on a 1.2%

agarose gel and visualized using ethidium bromide (data not shown). These successful results suggest that a significant cost savings may be obtained by using piezoelectric ink jet printing for the detection of clinically or environmentally relevant DNA species.

In general, globular proteins are stable in phosphate buffered saline with a small amount of non-denaturing detergent. We employed 1 % of polysorbate 20 surfactant, a detergent that is often used in protein purification due to its biochemical compatibility and protein stabilization (Sumerel et al., 2001). It has a second chemical attribute that it lowers the surface tension of the fluid. Bovine serum albumin was printed in 10 μ L drops, and then an α -BSA polyclonal antibody (Sigma Aldrich, St. Louis, MO) labelled with Cy3 was printed in random array over the protein drops. The protein array is shown where the antibody/antigen reaction is shown in green and protein alone is shown in blue (Figure 2).

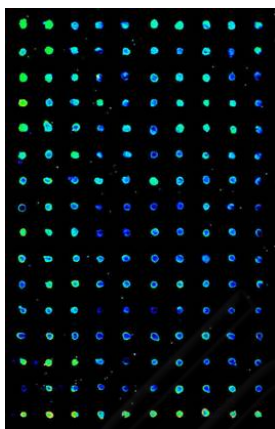


Figure 2: BSA protein incubated with α -BSA polyclonal antibody labelled with Cy3.

Due to appropriate fluid formulations required for ink jet printing, glycerol was added to the stock PEDOT/PSS solution to increase fluid viscosity. A waveform was employed for successful PEDOT/PSS printing (maximum jetting frequency of 1.0 kHz for a pulse width of 17.0 μ s). This waveform is a critical parameter for jetting this particular fluid.

The applied voltage was tuned specifically for each nozzle to provide uniform jetting speed to ensure reproducible drop volumes. Images of the jetting fluid were captured by light micrographs using this camera and software system (Figure 3).

In panel A, the fluid is leaving the nozzle with the ligament still evident. In panel B, at 500 μ m, the ligament has drawn into the drop, and the fluid is flying towards the substrate at 9.25 msec⁻¹, ten

times faster than the homebuilt printer discussed above (Teng and Vest, 1988). The resulting PEDOT/PSS on a silicon wafer pattern is shown (Figure 4). The PEDOT/PSS spreads on an untreated glass wafer with a contact angle of 18° (data not shown).

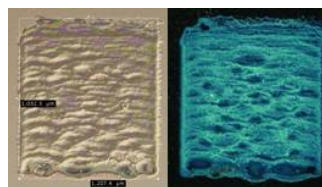


Figure 3: Light micrographs of fluid jetting from printhead nozzle and time of flights. A. Fluid leaving nozzle. B. Drop formation at 500 μ m.

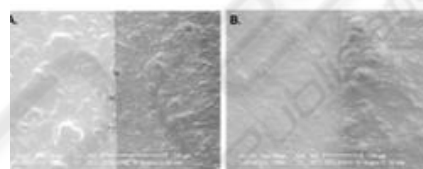


Figure 4: PEDOT/PSS printed on silicon wafer. A. Bright field. B. Dark field + UV.

Reliable printing procedures for two commercially available conductive silver precursors have been examined. Both fluids have ideal fluid flow properties for ink jet printing and have higher than 50% silver nanoparticle load. The viscosity and surface tension values of the ANP Silverjet nanopaste are 9 cps and 26.5 dynescm⁻¹ respectively. This fluid jetted at a maximum frequency of 5.0 kHz with a pulse width of 13.2 μ s.

Because of its high particle load (54%) and uniform particle size as demonstrated by transmission electron microscopy, low-temperature annealing produces a traceable conductivity in the printed material. Scanning electron micrographs were obtained of the annealed printed nanoparticles to compare the films produced (Figure 5).

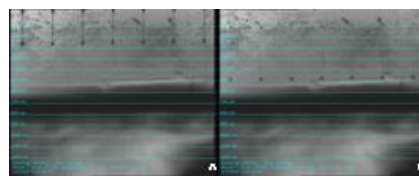


Figure 5: Electron micrographs of ANP silverjet nanopaste on Teslin®. Before annealing. B. After annealing.

Panel A shows the ANP Silverjet nanopaste on Teslin® before annealing (silver on left, Teslin® on right). With single-pass printing, the fluid makes a

uniform film on the Teslin[®] substrate in spite of the material's surface roughness (Panel A). Figure 5, panel B shows the same film on the same substrate after annealing for 1 hour at 200°C (annealed silver on left, Teslin[®] on right). Not only do the edges look slightly more uniform, but full coverage of the film on the substrate with single pass printing created a very thin silver full coverage film on the Teslin[®]. Because accurate feature measurements are difficult on flexible substrates, feature thickness was measured on gold-coated polished silicon nitride wafers (contact angle 41.8°, data not shown). We measured feature sizes using atomic force microscopy (AFM) with features printed at 20 mm drop spacing. Figure 6 shows the overall scan area of a single row of drops (Panel A).

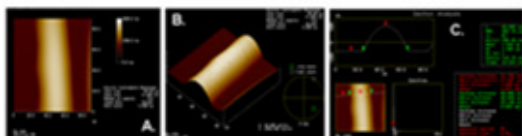


Figure 6: Atomic force microscope images of single row of ANP silver nanopaste drops. A. Overall scan area of a single row. B. 3D rendering C. Feature measurements.

The three-dimensional rendered view in Panel B shows the overall jetting uniformity. Panel C shows the calculated feature measurements. The width of the feature was 40.6 μm , and the film thickness of 1.59 μm demonstrates the utility of producing patterned thinfilms using ink jet printing technology. Because electrical performance is often described in terms of the bulk resistivity, resistance values were measured after annealing the silver nanoparticles. The resistance of the ANP Silverjet nanopaste is 1.1 Ω , and the resistance of the Cabot Inkjet Silver Conductor is 0.3 Ω (data not shown). The low resistance measurements in both cases were taken on equally-sized patterns on identical glass wafers. These values are in the same range as resistance values obtained by Sawhney and colleagues.

In order to achieve even finer features in manufacturing electronic applications, drop volumes below 10 μL are required. Employing 1 μL printheads, the reduced drop volume will produce 20 μm silver fluid features on Kapton[®] employing the ANP Silverjet nanopaste fluid. The miniaturization of drop volumes is demonstrated by ink jet printing with the 10 μL cartridge followed by ink jet printing with a 1 μL cartridge on the same wafer substrate and performing scanning electron microscopy (data not shown) where the radius of the 1 μL feature is more than twice as small as the radius of the 10 μL

feature. Smaller drop volumes will lead to fine conductive traces required for appropriate feature sizes in photovoltaic and electronic applications and directly address market demands.

Quantum dots were diluted in 53% polypropylene glycol 400, 45% propylene carbonate solution containing 0.01% tetramethyl-5-decyne-4,6-diol, 2,4,7,9-propanol and printed onto a clean silicon wafer (Figure 7) using an optimized waveform.

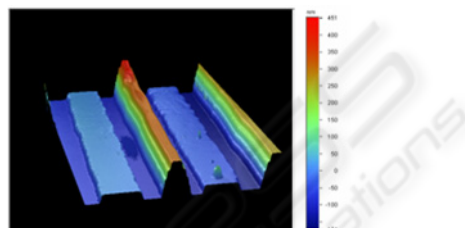


Figure 7: Scanning atomic force image of quantum dots printed on silicon wafer.

Although these particles are identical in synthesis methods and solvent composition, their concentration had a radical effect on their deposition on a silicon wafer substrate. The 2.6 nm quantum dots spread on the substrate whereas the 4.0 nm quantum dots did not spread to the same extent. The thinfilm produced by the 2.6 nm quantum dots was only 50 nm thick whereas the thinfilm produced by the 4.0 nm quantum dots was about 450 nm strongly suggesting that contributions to the final 3D structure of the thinfilm are particle-concentration dependent.

4 CONCLUSIONS

The software interface and waveform tuning allowed fluid process development for a scalable ink jet printing process. Ink jet printing of biologically active, electronic and semiconducting materials is a cost-effective manufacturing process. The printing parameters for these materials have been demonstrated, and the resulting interaction with the substrate demonstrates that ink jet printing is an iterative process where the interplay between the chemical properties of the fluid, the cartridge assembly, the machine operating procedure, the substrate and post-ink jet processing all determine whether this process is viable. Printing of two silver nanoparticle fluids has demonstrated the flexibility of the Dimatix Materials Printer, and these silver nanoparticles were successfully processed into conductive traces. Fluid formulation and ink jet

printing operating parameters are both key to the success of ink jet printing functional materials. Established operating parameters can now be translatable to production line systems with built in versatility, uniformity and scalability for biodevice production. Future directions will be to incorporate ink jet printing with circuit printing and biological fluid deposition for single deposition biodevice processing methods.

REFERENCES

- Antoniadis, H. Low-cost solar cells exploiting solar ink. in IEEE San Francisco Bay Area Nanotechnology Council Monthly meeting, 2007. Santa Clara, CA, USA.
- Bae, K.D., et al., Development of the new thermal head on SOI wafer. *Microelect. Eng.*, 2005. 78-79: p. 158-163.
- Baiesi, M., et al., Zipping and collapse of diblock copolymers. *Physical Review E*, 2001. 63: p. 41801-41811.
- Brünahl, J. and A.M. Grishij, Piezoelectric shear mode drop-on-demand ink jet actuator. *Sens. Act. A*, 2002, 101:371-382.
- Calvert, P., Ink jet printing for materials and devices. *Chem. Mater.*, 2001. 13: p. 3299-3305.
- Diehl, F., et al., Manufacturing DNA microarrays from unpurified PCR products. *Nucleic Acids Res.*, 2002. 30: p. 79-84.
- Grishij, Piezoelectric shear mode drop-on-demand ink jet actuator. *Sens. Act. A*, 2002. 101: p. 371-382.
- Haber, C., M. Boillat, and B. van der Schoot, Precise nanoliter fluid handling system with integrated high-speed flow sensor. *Assay Drug Dev Technol*, 2005. 3(2): p. 203-12.
- Hwang, J.S., Solder materials and process for electronic assembly fabrication, in *Electronic Assembly Fabrication, chips, circuit boards, packages and components*, C.A. Harper, Editor. 2002, McGraw-Hill: New York, NY. p. 305-362.
- Lemmo, A.V., D.J. Rose, and T.C. Tisone, Ink jet dispensing technology: applications in drug discovery. *Curr. Opin. Biotechnol.*, 1998. 9: p. 615-617.
- Lewis, J.A., et al., Direct ink writing of three-dimensional ceramic structures. *J. Am. Ceram. So*, 2006. 89: p. 3599-3609.
- Manning, H., Application of ink jet technology for microarrays and other bio printing, in *Bioprinting*. 2007: London, England.
- Mei, J., M.R. Lovell, and M.H. Mickle, Formulation and processing of novel conductive solution inks in continuous ink jet printing of 3-D electric circuits. *IEEE Trans. Electron. Packag. Manuf.*, 2005. 28: p. 265-273.
- Menzel, C. MEMS solutions for precision micro-fluidic dispensing application. in *NIP20: International Conference on Digital Printing Technologies*. 2005. Salt Lake City Utah.
- Myatt, C., N. Traggis, and K.L. Dessau, Optical fabrication: optical contacting grows more robust. *Laser Focus World*, 2006. 42: p. 95-98.
- Padinger, F., Biosensors and printed electronics for life sciences, in *Bioprinting 2007: London, England*.
- Peck, W., in-situe microarray manufacturing using ink jet technology at Agilent Technologies, in *Bioprinting*. 2007: London, England.
- Rodriguez-Calvo, M.S., et al., Isoelectric focusing of human hair keratins: correlation with sodium dodecyl sulfate-polyacrylamide gel electrophoresis (SDS-PAGE): patterns and effect of cosmetic treatments. *J. Forensic Sci.*, 1992. 37: p. 425-431.
- Salas, A., et al., Fluorescent SSCP of overlapping fragments (FSSCP-OF): a highly sensitive method for the screening of mitochondrial DNA variation. *Forensic Sci. Inter.*, 2001. 124: p. 97-103.
- Setti, L., et al., An amperometric glucose biosensor prototype fabricated by thermal ink jet printing. *Biosensors and Bioelectronics*, 2005. 20: p. 2019-2026.
- Sawhney, A., et al., Piezoresistive sensors on textiles by ink jet printing and electroless plating. *Mater. Res. Symp. Proc.*, 2006. 920: p. 4-13.
- Shaw, J.M. and P.F. Seidler, Organic electronics: Introduction. *IBM Journal of Research and Development*, 2001. 45(1): p. 3-10.
- Sirringhaus, H., et al., High-resolution ink jet printing of all-polymer transistor circuits. *Science*, 2000. 290(5499): p. 2123-6.
- Song, J.H. and H.M. Nur, Defects and prevention in ceramic components fabricated by ink jet printing. *Mater. Proc. Technol.*, 2004. 155: p. 1286-1292.
- Sumerel, J., et al., Cyclin E and its associated cdk activity do not cycle during early embryogenesis of the sea urchin. *Dev Biol.*, 2001. 234(2): p. 425-40.
- Sumerel, J., et al., Piezoelectric ink jet processing of materials for medical and biological applications. *Biotechnol J*, 2006. 1(9): p. 976-87.
- Teng, K.F. and R.W. Vest, Metallization of solar cells with ink jet printing and silver metallo-organic inks. *IEEE Trans. Compon. Hyb. Manuf. Tech.*, 1988. 11: p. 291-297.
- Volkman, S.K., et al., Ink-jetted silver/copper conductors for printed RFID applications. *Mat. Res. Soc. Symp. Proc.*, 2004. 814: p. 1-6.
- Vuorio, A.F., et al., Amplification of the hypervariable region close to the apolipoprotein B gene: application to forensic problems. *Biochem. Biophys. Res. Comm.*, 1990. 170: p. 616-620.
- Wilson, M.R., et al., Validation of mitochondrial DNA sequencing for forensic casework analysis. *Int. J. Legal. Med.*, 1995. 108: p. 68-74.
- Xu, T., et al., Ink jet printing of viable mammalian cells. *Biomaterials*, 2005. 26(1): p. 93-9.